Eur Radiol (2002) 12:2335–2338
DOI 10.1007/s00330-002-1310-9

M. Uhl
C. Altehoefer
U. Kontny
K. Il'yasov
M. Büchert
M. Langer

MRI-diffusion imaging of neuroblastomas: first results and correlation to histology

Received: 18 June 2001
Revised: 19 November 2001
Accepted: 7 December 2001
Published online: 19 March 2002
© Springer-Verlag 2002

M. Uhl (✉)
Section of Paediatric Radiology,
University Hospital Freiburg,
Hugstetterstrasse 55, 79106 Freiburg,
Germany
e-mail: UHL@MRS1.UKL.uni-freiburg.de
Tel.: +49-761-2703940
Fax: +49-761-2703942

C. Altehoefer · U.Kontny
Children's Hospital,
University Hospital Freiburg,
Hugstetterstrasse 55, 79106 Freiburg,
Germany

K. Il'yasov · M. Büchert
Section of MR Physics,
University Hospital Freiburg,
Hugstetterstrasse 55, 79106 Freiburg,
Germany

M. Langer
Department of Diagnostic Radiology,
University Hospital of Freiburg,
Hugstetterstrasse 55, 79106 Freiburg,
Germany

Abstract The purpose of this study was to evaluate diffusion-weighted MR imaging in neuroblastomas. We prospectively examined seven children (age range 1–3 years) with seven solid body neuroblastomas. Diagnosis was established histologically. Diffusion-weighted echo-planar imaging (EPI) sequence was performed in all patients, with a repetition time of 5400 ms and an echo time of 103 ms, and with a b-value of 1000 s/mm^2. The contrast of tumour tissue depicted with T2-weighted images and diffusion-weighted images were evaluated by means of region-of-interest measurements and a calculation of the apparent diffusion coefficient (ADC) was done. The ADC calculation showed a mean ADC of 1.1×10^{-3} (SD 0.14×10^{-3}, range $0.9–1.2\times10^{-3}$) mm^2/s of all tumours. Diffusion-weighted images showed an increased tumour signal. Water proton diffusion within the tumour matrix of neuroblastomas is especially restricted by the molecular and macromolecular barriers due to the very dense structure of this tumour tissue. We hypothesize that high nuclear-to-cytoplasm ratio of neuroblastoma cells limits intracellular motion. Furthermore, the very densely packed tumour cells inhibit effective motion of extracellular water protons. Restricted proton motion leads to a reduction in the rate of apparent diffusion and to a marked increase in signal on diffusion-weighted EPI MR images.

Keywords Magnetic resonance · Comparative studies · Diffusion study · Histology correlation · Tumour diagnosis · Neuroblastoma diagnosis

Introduction

Diffusion-weighted MR imaging is a concept that was introduced as intravoxel incoherent motion by Le Bihan et al. [1, 2]. Diffusion-weighted imaging depicts differences in molecular diffusion and local water mobility [3, 4]. Molecular diffusion is a process of water molecules spontaneously moving along random pathways, the so-called Brownian motion [6, 7, 8].

Tissue characterization of tumours using MRI depends basically on T1- and T2-relaxation times (signal intensities) and contrast-medium enhancement. Considerable interest came up concerning the ability of MRI to image and measure molecular diffusion. The interest in diffusion results from the unique feature of this parameter: diffusion directly reflects molecular mobility and molecular motion [1, 2]; thus diffusion represents a possible parameter in tissue characterization. The apparent

diffusion coefficient (ADC) of water in tissue is two or three times less than its value in pure water [1, 2]. This is largely explained by the high viscosity of bulk water in tissue because of the presence of large molecules such as proteins in intracellular space which represent obstacles to molecular diffusion. Tissues (normal or abnormal) with different viscosities or a different balance between intracellular and extracellular water thus present different diffusion coefficients, the source of contrast in diffusion imaging [1, 7, 9, 10, 12, 16]. Characterization of tumour tissue may benefit from molecular mobility measurements.

Neuroblastoma is the most common extracranial solid tumour of childhood, accounting for 8–10% of all childhood cancers. The median age at diagnosis is 2 years. Neuroblastomas originate in neural crest cells of the sympathetic nervous system and thus develop anywhere from the posterior cranial fossa to the coccyx. Approximately 70% of the tumours arise in the abdomen. Histologically, this highly malignant tumour consists of small round cells, whereas most tumours consist of primitive neuroblastoma cells with little evidence of differentiation [5, 13].

The aim of our study was therefore to evaluate diffusion-weighted imaging studies of neuroblastomas in comparison with standard T1- and T2-weighted MRI pulse sequences.

Patients and methods

Prospectively we examined seven children (five girls, two boys; age range 1–3 years, mean age 1.6 years) with seven solid neuroblastomas. All tumours were biopsied after an MRI examination and diagnosis was established histologically.

We found five neuroblastomas of the thoraco-abdominal sympathetic nervous system and two tumors of the adrenal gland. The average size of all tumors was 80 ml tissue volume (range 15–150 ml).

The MR imaging was performed with a 1.5-T system (Vision, Siemens, Erlangen, Germany) with body coil or standard head coil (children with body weight <10 kg). Five- to 8-mm-thick transversal T1-weighted spin-echo sequences (SE) were acquired with TR=450 ms and TE=12 ms, two excitations and 256×256 matrix. Transversal T2-weighted turbo-spin-echo (TSE) images were obtained with TR/TE=3600/120 ms; echo train length=7, two excitations and 256×256 matrix. A T1-weighted sequence was repeated after intravenous injection of 0.1 mmol of gadopentetate dimeglumine (Magnevist, Schering, Berlin, Germany) per kilogram of body weight.

Diffusion-weighted echo-planar imaging (EPI) sequence was performed in all patients, with a TR of 5400 ms and a TE of 103 ms, and a b-value of 0 and 1000 s/mm^2. This high diffusion weighting is very sensitive to diffusional motions. As diffusion is an orientation-dependent phenomenon, all images were obtained in three perpendicular axes (x, y and z) to notice anisotropic imaging effects. Slice thickness of these diffusion-weighted, transversal images was 8 mm, and matrix was 230×230. Eight slices were gained.

Two experienced radiologists evaluated signal intensity characteristics in tumour tissue on all MRI sequences qualitatively. Signal intensities of the tumour tissues were classified as hypo-, iso- or hyperintense to the muscle signal intensity. The contrast of tumour tissue vs muscle tissue depicted with T2-weighted images and diffusion-weighted images were evaluated by means of region-of-interest measurements. The regions of interest were placed in tumour tissue, in adjacent muscle tissue without signal abnormalities, and in background noise. Contrast ratios were determined as follows: $(SI_A\text{-}SI_N)/SI_N$, where SI_A is the signal intensity of abnormal tissue and SI_N the signal intensity of adjacent muscle tissue. Tumour necrosis was defined as lesion within a tumour with a very high signal on T2-weighted images, and lack of enhancement after i.v. contrast administration.

Apparent diffusion coefficient (ADC) of the tumour and normal muscle tissue was calculated using the following formula:

$$ADC=[\ln (So/S1)]/(b1\text{-}bo),$$

where S0=signal intensity b=0, and S1=signal intensity b=1000) [4]. We calculated the signal intensities using a region of interest in the centre of tumour tissue with an area of 50×50 pixels. Sufficient ADC mapping was not possible due to motion- and susceptibility artifacts which leads to image distortion.

Results

All neuroblastomas were hyperintense on diffusion-weighted images (Fig. 1d). Six of seven neuroblastomas had hyperintense signal behaviour on T2-weighted images (one neuroblastoma was only slightly hyperintense on the T2-weighted image). In seven neuroblastomas, T1-weighted images depicted isointense tumour masses (Table 1). All tumours showed a moderate inhomogeneous contrast enhancement after i.v. gadolinium-DTPA.

Contrast ratios of all tumours on T2-weighted images were lower (1.7; SD 2.0) than on diffusion-weighted images (mean 6.3; SD 3.3). One neuroblastoma had a necrotic–ischaemic area. This lesion had a high signal on T2-weighted images and a lack of enhancement after i.v. contrast application. On diffusion-weighted images, this necrotic area within the tumour showed an impressive loss of signal.

The ADC calculation showed a mean ADC of 1.8×10^{-3} (SD 0.14×10^{-3}, range $0.9\text{–}2.1\times10^{-3}$) mm^2/s of all tumours. The ADC value of muscle tissue was 0.29×10^{-3} (SD 0.1×10^{-3}) mm^2/s.

Table 1 Distribution of signal intensities of neuroblastomas as compared with muscle. One neuroblastoma was only slightly hyperintense on the T2-weighted MR image

Tumours	Signal intensities			
	Hyperintense	Isointense	Hypointense	Σ
T1	0	7	0	7
T2	6	1	0	7
Diffusion	7	0	0	7

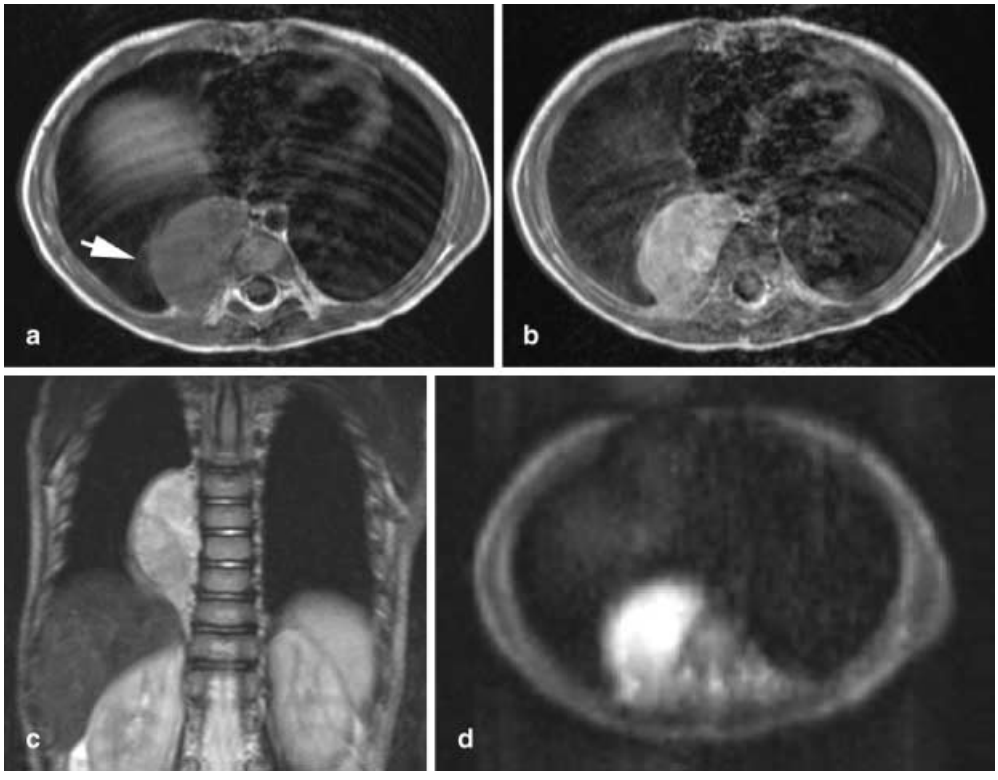

Fig. 1a–d Neuroblastoma (*arrow* in **a**) in a 2-year-old boy. **a** T1-weighted spin echo (SE) image (TR/TE: 450 ms/12 ms). **b** T1-weighted SE after i.v. gadolinium-DTPA 0.1 mmol/kg body weight. **c** T2-weighted turbo SE (TR/TE/echo train length: 3600 ms/120 ms/7). **d** Echo-planar diffusion-weighted image. Note the hyperintense appearance of the tumour in the diffusion-weighted imaging (TR/TE: 5400 ms/103 ms; b=1000)

Discussion

To our knowledge, this is the first study of signal behaviour using diffusion-weighted MR imaging of a typical paediatric body tumour. We postulate that water proton diffusion within the tumour matrix of neuroblastomas is restricted by molecular and macromolecular barriers due to the very dense structure of the tumour tissue (Fig. 2). The high nuclear-to-cytoplasm ratio of these tumour cells limits intracellular motion [8]. The very densely packed and randomly organized tumour cells inhibit the effective motion of extracellular water protons (see Fig. 1, diffusion-weighted image). Restricted proton motion leads to a reduction in the rate of apparent diffusion and to a marked increase in the signal on diffusion-weighted MR images. Other tumours with extraordinarily densely packed cells are also high-grade gliomas and medulloblastomas (Fig. 3).

Indeed, the diffusion-weighted imaging of these tumours are similar, in contrast to those of other brain tumours [8, 14].

We hypothesise that tumours with high-signal appearance on conventional T2-weighted images and a high signal on diffusion-weighted images (or ADC maps) are lesions with densely packed cells. Malignant lymphomas have such characteristics, and one case report of a central nervous system lymphoma [15] supports this supposition. On the other hand, lesions with high signal intensities on T2-weighted images and low signal intensity on diffusion-weighted images are tumours with low cellularity [11], e.g. cysts and necrotic portions of tumours. The combination of hyperintense and hypointense sig-

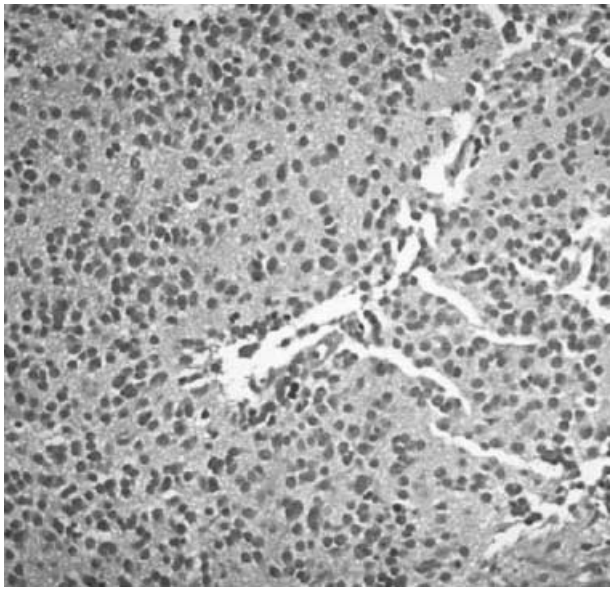

Fig. 2 Histological specimen shows small, round, densely packed tumour cells of a typical neuroblastoma

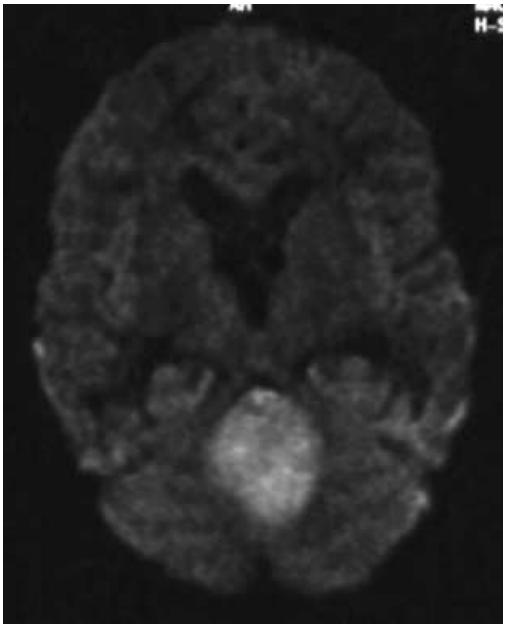

Fig. 3 Echo-planar diffusion-weighted image of a typical medulloblastoma of the brainstem in a 4-year-old girl. Corresponding to the histology of neuroblastomas, densely packed small tumor cells are responsible for diffusion loss in that tumor, too

nals on diffusion-weighted images was seen in haemorrhagic tumours, as reported by Okamato et al. [11].

Different diffusion-weighted sequences have been described, including SE, EPI, and steady-state free precession sequences (SSFP, CE-Fast). The disadvantages of the SE method are long acquisition times and vulnerability to motion artefacts. Steady-state sequences do not permit precise calculations of the b-value in vivo, which represents diffusion strength [4]. The EPI sequences can be performed within a few seconds, and thus with reduced motion artefacts. The disadvantage of EPI is high sensitivity to susceptibility, which leads to image distortion and signal loss. We found that EPI sequences were very useful in our paediatric population due to short acquisition time and limited motion artefacts.

In conclusion, we present seven proven cases of neuroblastomas and propose that the small cell histology of this tumour is appropriate to explain signal characteristics on diffusion-weighted imaging. We propose diffusion-weighted imaging in paediatric patients as a tool for differential diagnosis of abdominal tumours. Furthermore, diffusion-weighted imaging seems useful as an imaging tool for more precise demarcation of tumour tissue.

References

1. Le Bihan D, Breton E, Lallemand D, Laval-Jeantet M (1986) MR imaging of intravoxel incoherent motions: application to diffusion and perfusion in neurologic disorders. Radiology 161:401–405
2. Le Bihan D (1992) Diffusion and perfusion. In: Stark D, Bradley WG (ed) Magnetic resonance imaging. Mosby, St. Louis, p 335
3. Baur A, Staebler A, Bruening R, Deimling M (1998) Diffusion-weighted MR imaging of bone marrow: differentiation of benign versus pathologic compression fractures. Radiology 207:349–356
4. Baur A, Reiser M (2000) Diffusion weighted imaging of the musculoskeletal system in humans. Skelet Radiol 29:555–562
5. Brodeur G, Castleberry R (1997) Neuroblastoma. In: Pizzo PA, Poplack DG (ed) Principles and practice of pediatric oncology. Lippincott, Philadelphia, p 480
6. Debaere C, Stadnik T, De Maeseneer M, Osteaux M (1999) Diffusion-weighted MRI in cyclosporin A neurotoxicity for the classification of cerebral edema. Eur Radiol 9:1916–1918
7. Kluytmans M, van Everdingen KJ, Kapelle LJ, Ramos LM, Viergever MA, van der Grond J (2000) Prognostic value of perfusion- and diffusion weighted MR imaging in first 3 days of stroke. Eur Radiol 10:1434–1441
8. Kotsenas A, Roth T, Maness W, Faerber E (1999) Abnormal diffusion-weighted MRI in a medulloblastoma: Does it reflect small cell histology? Pediatr Radiol 29:524–526
9. Lang P, Johnston JO, Arenal-Romero F, Gooding CA (1998) Advances in MR imaging of pediatric musculoskeletal neoplasms. Magn Reson Imaging Clin North Am 6:579–581
10. Lang P,Wendland MF, Sead M et al. (1998) Osteogenic sarcoma: noninvasive in vivo assessment of tumor necrosis with diffusion-weighted MR imaging. Radiology 206:227–235
11. Okamato K, Ito J, Ishikawa K, Sakai K, Tokiguchi S (2000) Diffusion-weighted echo-planar MR imaging in differential diagnosis of brain tumors and tumor-like conditions. Eur Radiol 10:1342–1350
12. Uhl M, Hauer M, Allmann KH, Gufler H, Laubenberger J, Hennig J (1998) New developments in MRI sequences. Akt Radiol 8:4–8
13. Santana V (1996) Neuroblastoma. In: Behrmann R, Kliegman R, Arvin A (ed) Textbook of pediatrics. Saunders, Philadelphia, p 1460
14. Tien R, Felsberg G, Freidman H et al. (1994) MR imaging of high grade gliomas: value of diffusion-weighted echo planar sequences. Am J Roentgenol 162:671–677
15. Wang AM, Shetty AN, Woo H et al. (1998) Diffusion weighted MR imaging in evaluation of CNS diseases. XVI. Symposium Neuroradiologicum, 36th annual meeting of the ASNR, Philadelphia, May 1998
16. Wiemann M, Mayer TE, Yousry I, Hamann GF, Bruckmann H (2001) Detection of hyperacute parenchymal hemorrhage of the brain using echo-planar T2-weighted and diffusion-weighted MRI. Eur Radiol 11:849–853